J Mater Sci: Mater Electron
DOI 10.1007/s10854-017-7163-4

Novel temperature stable $Ba_{1-x}Sr_xV_2O_6$ microwave dielectric ceramics with ultra-low sintering temperature

Guo-Guang Yao[1] · Cui-Jin Pei[1] · Peng Liu[2] · Hui-Yu Xing[1] · Long-Xi Fu[1] · Bai-Cheng Liang[1]

Received: 4 April 2017 / Accepted: 15 May 2017

Abstract New temperature stability $Ba_{1-x}Sr_xV_2O_6$ ($0.35 \le x \le 0.55$) microwave dielectric ceramics prepared by the conventional solid-state route were investigated. X-ray diffraction confirmed that all the specimens formed a solid solution single phase with orthorhombic structure. The microwave dielectric properties strongly depended on the compositions, densification and microstructure of the specimens. Furthermore, partial Sr ions substitution for Ba ions in $Ba_{1-x}Sr_xV_2O_6$ lattices not only successfully improved the temperature stability of BaV_2O_6-based ceramic but also promoted the sinterability of SrV_2O_6-based one. Out of these compositions, $Ba_{0.5}Sr_{0.5}V_2O_6$ sintered at 625 °C exhibited a near-zero τ_f together with a low permittivity $\varepsilon_r \sim 11.5$ and a quality factor $Q \times f \sim 14\,100$ GHz, which also showed good chemical compatibility with Al electrodes.

1 Introduction

In recent years, enormous research has been devoted to seeking microwave dielectric ceramics with low permittivity (ε_r), high quality factor ($Q \times f$), and a near-zero temperature coefficient of resonant frequency (τ_f), which are widely used for high-frequency devices. Besides, the requirement for miniaturized and performance-enhanced microwave devices for use in microwave communication systems has increased [1–3]. Such requirements can be met by employing low-temperature co-fired ceramic (LTCC) technology to enable the fabrication of multilayer devices [4]. Moreover, the latest trend in LTCC technology is to develop new dielectrics with ultra-low sintering temperature ($Ts < 650$ °C) to save energy, protect environment, and to enable further seamless integration with silicon technology, metals or even organic substrates [5, 6]. The continuous efforts in this aspect have led to a new class of materials known as ultra-low-temperature co-fired ceramics (ULTCC), wherein the base ceramic composition sinters at temperatures lower than the melting point of the electrode material, i.e. aluminum (660 °C) [7–10].

Recently extensive efforts have been made in vanadate compounds to identify novel microwave ceramic systems suitable for application in LTCC substrate since they possess low or even ultra-low sintering temperature and excellent microwave dielectric properties [11–17]. In $BaO–V_2O_5$ binary system, five phases are formed: $Ba_3(VO_4)_2$, $Ba_2V_2O_7$, $Ba_3V_4O_{13}$, $Ba_{16}V_{18}O_{61}$ and BaV_2O_6 [18–22]. All of them not only show good microwave dielectric properties ($\varepsilon_r = 9.6 \sim 17$, $Q \times f = 21\,800 \sim 80{,}100$ GHz and $\tau_f = -64 \sim 40$ ppm/°C) but also own inherently low or ultra-low sintering temperature, except for $Ba_3(VO_4)_2$ ($Ts = 1600$ °C). In particular, the orthorhombic structure BaV_2O_6 ceramic is of special interest due to its exceptionally relatively low ε_r but a large positive τ_f value (40 ppm/°C) as well as good chemical compatibility with Al electrode. However, it is the large positive τ_f value restricted its further application. Ion substitution is an effective method to improve or compensate the dielectric properties of ceramics by forming a solid solution or composite materials [23]. It was previously revealed that the substitution of smaller Sr ions (0.69 Å, CN = 6) for Ba ions

✉ Guo-Guang Yao
yaoguoguang@xupt.edu.cn

✉ Peng Liu
liupeng@snnu.edu.cn

[1] School of Science, Xi'an University of Posts and Telecommunications, Xi'an 710121, China

[2] College of Physics and Information Technology, Shaanxi Normal University, Xi'an 710062, China

Published online: 19 May 2017

(0.74 Å, C = 6) contributed to the increase of the A-site bond valence in the tetragonal structured $Ba_{1-x}Sr_xMg_2V_2O_8$ system, which resulted in that the τ_f values varied from negative to positive [24]. SrV_2O_6 shows the same crystal structure with that of BaV_2O_6 [25]. Thus, a near-zero τ_f may be obtained by preparing Ba_{1-x} $Sr_xV_2O_6$ solid solution ceramics. In this work, the Ba_{1-x} $Sr_xV_2O_6$ solid solution ceramics were prepared and a detailed investigation was performed to provide an insight into the relations between the structure and the microwave dielectric properties. As expected, the desired dielectric properties, was the result of a simple optimization of the $Ba_{1-x}Sr_xV_2O_6$ compositional parameters as well as the sintering condition. Furthermore, the chemical compatibility between $Ba_{0.5}Sr_{0.5}V_2O_6$ ceramics and Al electrodes was also investigated.

2 Experimental Procedure

The starting materials are high-purity oxide powders (>99.9%; Guo-Yao Co. Ltd., Shanghai, China): $BaCO_3$, $SrCO_3$, and V_2O_5. Predried raw materials were separately weighed in stoichiometric mixtures $Ba_{1-x}Sr_xV_2O_6$ ($0.35 \le x \le 0.55$) and ball-milled for 8 h in a nylon jar with agate balls and ethanol as media. The resultant slurry was dried, then ground well, and calcined at 500 °C for 3 h. The calcined powders were reground for 8 h, dried, mixed with 5 wt% polyvinyl alcohol (PVA) as a binder, and granulated. The granulated powders were uniaxially pressed into pellets 10 mm in diameter and 5 mm in thickness under a pressure of 100 MPa. These pellets were sintered from 575 to 650 °C for 4 h in air with a heating rate of 5 °C/min, and then cooled to room temperature.

Table 1 The cell parameters and cell volume of the $Ba_{1-x}Sr_xV_2O_6$ ceramics sintered at 625 °C for 4 h

Compounds	Cell	Parameter (Å)		Cell volume (Å^3)
	a	b	c	
$Ba_{0.65}Sr_{0.35}V_2O_6$	8.4125	12.5441	7.8373	827.0486
$Ba_{0.6}Sr_{0.4}V_2O_6$	8.3791	12.5519	7.8353	824.0699
$Ba_{0.5}Sr_{0.5}V_2O_6$	8.3666s	12.5171	7.8011	816.9746
$Ba_{0.45}Ca_{0.55}V_2O_6$	8.3851	12.4902	7.7827	815.0944

The bulk densities of the sintered ceramics were measured by Archimedes' method.

The crystal structures were analyzed using powder X-ray diffraction (XRD) with Cu Ka radiation (Rigaku D/MAX2550, Tokyo, Japan). The microstructure of pellets was investigated using a scanning electron microscope (SEM, Fei Quanta 200, Eindhoven, Holland) coupled with energy dispersive X-ray spectroscopy (EDS). The microwave dielectric properties of sintered samples were measured using a network analyzer (ZVB20, Rohde and schwarz, Munich, Germany) with the $TE_{01\delta}$ shielded cavity method. The temperature coefficient of resonant frequency (τ_f) was calculated with the following Eq. (1):

$$\tau_f = \frac{f_{80} - f_{20}}{f_{20} \times (80 - 20)} \quad (1)$$

where f_{80} and f_{20} are the resonant frequency at 80 and 20 °C, respectively.

3 Results and discussion

Figure 1 shows the XRD patterns for $Ba_{1-x}Sr_xV_2O_6$ ceramics (x = 0.35–0.55) sintered at 625 °C. All peaks could be attributed to orthorhombic phases (JCPDS #34−0014), indicating a single-phase continuous solid solution was formed for all the compositions. Diffraction peaks shifted to higher diffraction angle with increasing Sr concentration, consistent with the differences in the ionic radius of Ba^{2+} (1.61 Å) and Sr^{2+} (1.44 Å) ions, and the corresponding cell parameters and cell volume of the $Ba_{1-x}SxV_2O_6$ ceramics are illustrated in Table 1. Density and microwave dielectric properties of the $Ba_{1-x}SxV_2O_6$ ceramics system sintered at 625 °C for 4 h are summarized in Table 2. As x increased from 0.35 to 0.55, the τ_f values decreased from 9.0 to −10.0 ppm/°C and a near-zero τ_f could be obtained for $Ba_{0.5}Sr_{0.5}V_2O_6$ specimen. This change indicated that the SrV_2O_6 ceramics should have negative τ_f. However, the microwave dielectric properties of the SrV_2O_6 ceramics have not been reported so far. Thus, the SrV_2O_6 ceramics has been prepared separately and its truly exhibited negative τ_f value (about −50.0 ppm/°C) after sintering at optimum temperature of 550 °C.

Table 2 Density and microwave dielectric properties of Ba_{1-x} $Sr_xV_2O_6$ ceramics sintered at 625 °C for 4 h

Compounds	Theoretical density (g/cm3)	Relative density (%)	ε_r	Q × f (GHz)	τf (ppm/°C)
$Ba_{0.65}Sr_{0.35}V_2O_6$	3.830	94.5	11.2	13 600	9.0
$Ba_{0.6}Sr_{0.4}V_2O_6$	3.814	96.5	11.8	14 900	6.0
$Ba_{0.5}Sr_{0.5}V_2O_6$	3.786	96.3	11.5	14 100	−3.5
$Ba_{0.45}Sr_{0.55}V_2O_6$	3.764	92.5	9.3	13 700	−10.0

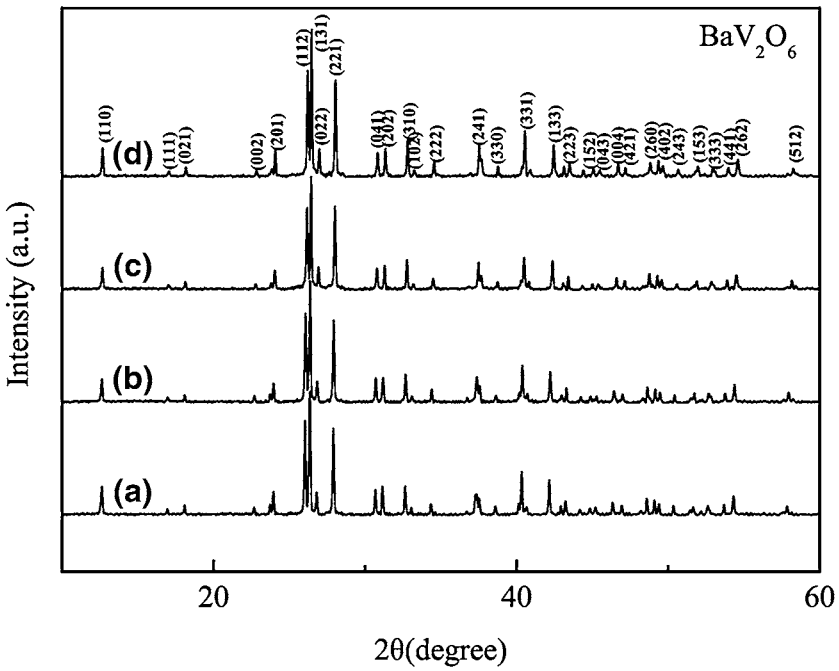

Fig. 1 XRD patterns for $Ba_{1-x}Sr_xV_2O_6$ ceramics sintered at 625 °C: **a** x = 0.35, **b** x = 0.4, **c** x = 0. 5, and **d** x = 0.55

The XRD patterns of the $Ba_{0.5}Sr_{0.5}V_2O_6$ ceramics sintered at different temperatures are displayed in Fig. 2. No structural change and secondary phase were observed in all sintering temperatures. This means that the stable structure of $Ba_{0.5}Sr_{0.5}V_2O_6$ could be obtained in sintering temperature range of 575–650 °C. Moreover, with increasing sintering temperature from 575 to 650 °C, the main peak (131) firstly shifted to low angle and then to high angle, accompanied with the intensity changes both (041) and (202) peaks. This change indicated the $Ba_{0.5}Sr_{0.5}V_2O_6$ ceramics could self-adjust cell unit, depending on the firing temperature [26], which may be related to the evaporation of V, as evidenced by SEM analysis below.

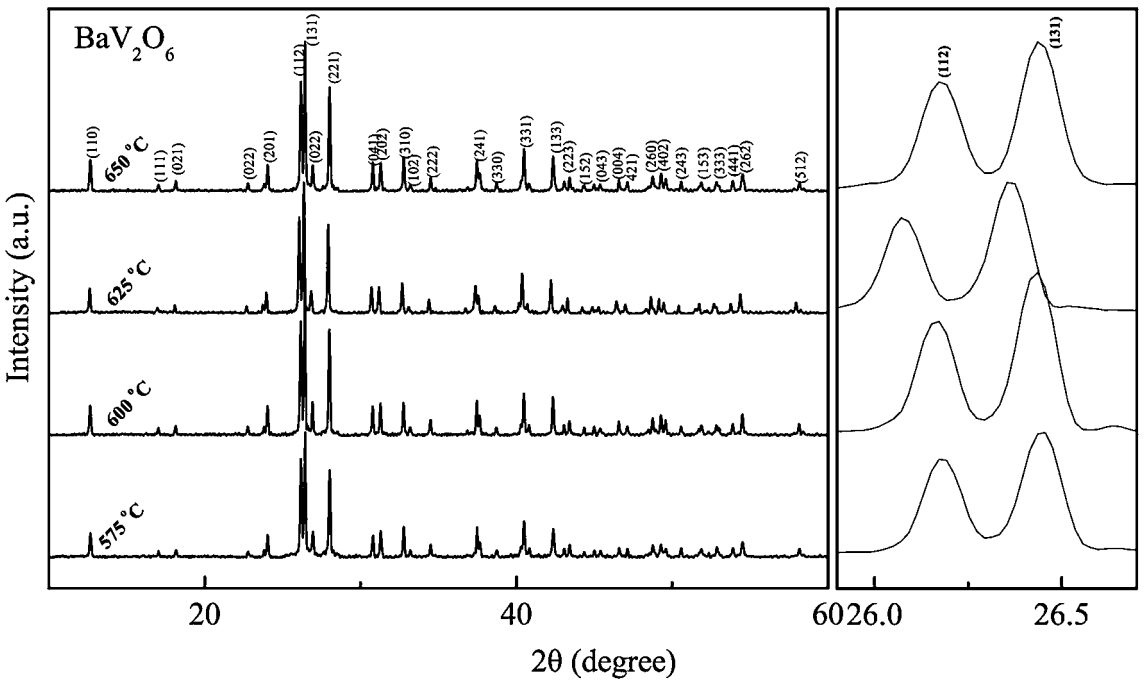

Fig. 2 XRD patterns of the $Ba_{0.5}Sr_{0.5}V_2O_6$ ceramics sintered at different temperatures

Figure 3 demonstrates the typical SEM images of the $Ba_{0.5}Sr_{0.5}V_2O_6$ ceramics fired at different temperatures. From (a) to (c), the grain size and homogeneity increased as the firing temperature raised from 575 to 625 °C, and the relatively homogenous microstructures could be obtained for the samples sintered at 625 °C, which may anticipate improved the microwave dielectric properties. However, the microstructure of the ceramic sintered above 625 °C exhibited formation of abnormal large grains, partial melting of grains and cracks, which may deteriorate the microwave dielectric properties of ceramics. Moreover, the inset of Fig. 3c shows the SEM image of the fracture surface of the $Ba_{0.5}Sr_{0.5}V_2O_6$ ceramics sintered at 625 °C. The fracture surface revealed some pores inside the grains caused by vanadium evaporated from the sample during the sintering process, which supported the XRD results discussed above.

The bulk density and microwave dielectric properties of the $Ba_{0.5}Sr_{0.5}V_2O_6$ ceramics sintered at different temperatures are shown in Fig. 4. The bulk density decreased from 3.796 to 3.453 g/cm^3 with increasing sintering temperature from 575 to 650 °C, which is due to the increase of the content of vanadium volatilization and oxygen vacancies [27, 28]. Thus, it is difficult to estimate the relative densities in the $Ba_{0.5}Sr_{0.5}V_2O_6$ ceramics because VO_5 is evaporated during sintering. As well known, the variation of the concentration of polarized particles in a unit volume will result in the decline or rise of the relative dielectric constant. Pores, oxygen vacancies and evaporation of elements (such as V^{5+}) are the key factors to inhibit the concentration of polarized particles per volume [27]. A higher density for a ceramic body means there are more polarized particles in a unit volume and the ceramic is easier to be polarized. In the present case, the variation of ε_r value with sintering temperature showed the same trend as that of density, indicating that the density was the dominating factor to control ε_r. As shown in Fig. 4b, with increasing sintering temperature, the Q×f value initially increased and then declined after reaching a peak value. Generally speaking, the Q×f for given ceramics dependents on the extrinsic factors, such as density, impurity, crystal defects, secondary phase

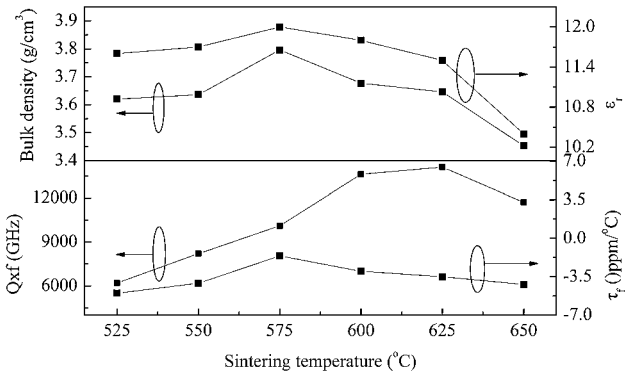

Fig. 4 The bulk density and microwave dielectric properties of the $Ba_{0.5}Sr_{0.5}V_2O_6$ ceramics sintered at different temperatures

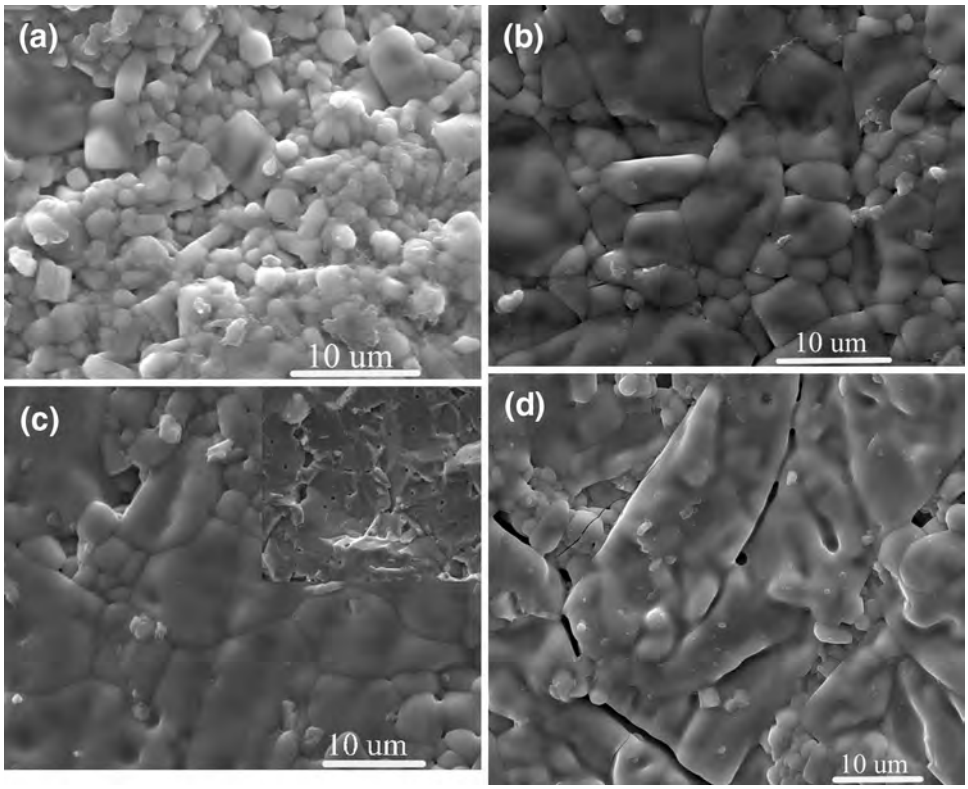

Fig. 3 Typical SEM images of the $Ba_{0.5}Sr_{0.5}V_2O_6$ ceramics fired at different temperatures: **a** 575, **b** 600, **c** 625, and **d** 650 °C. The *inset* of **c** shows the corresponding fracture surface image

and grain size [29]. Combined with the results of XRD, SEM and density, the improvement of Q×f was due to the decrease of grain boundaries as well as the incensement of density, apart from secondary phase. This is because of that grain boundary could act as a two-dimension defect disturbing the symmetry of the crystal, and then high Q×f would be influenced [30]. The decrease of Q×f value was attributed to over-sintering, resulting in the poor microstructure as illustrated in Fig. 3d. As shown in Fig. 4b, the τf values slightly decreased from −1.5 ppm/°C to −5.0 ppm/°C as the sintering temperatures changed. Hong et al. [31] reported that τ_f is inversely proportional to the unit-cell volume if compounds are same structure. Moreover, Rout et al. [32] revealed that the porosity is also known to have an effect on the τ_f values of ceramics. Therefore, we believe the above two factors combined are responsible for the slight variation in τ_f values of $Ba_{0.5}Sr_{0.5}V_2O_6$ ceramics with increasing sintering temperature.

The chemical compatibility of ULTCC material with Al is of major concern for practical applications. Therefore, it is necessary to study the reactivity of $Ba_{0.5}Sr_{0.5}V_2O_6$ ceramics with Al, to evaluate its potential as ULTCC materials. Figure 5 presents the XRD patterns and cross-section SEM image of the $Ba_{0.5}Sr_{0.5}V_2O_6$ ceramics after co-firing with 20 wt% Al at 625 °C for 5 h. As shown in Fig. 5, only peaks of Al, and $Ba_{0.5}Sr_{0.5}V_2O_6$ phases could be separately identified and no additional peaks were revealed. Meanwhile, as seen in the inset of Fig. 5, no chemical reaction or diffusion and good contact at interface of $Ba_{0.5}Sr_{0.5}V_2O_6$ and Al electrode were observed from the SEM image. Both the XRD and SEM analysis results confirmed that the $Ba_{0.5}Sr_{0.5}V_2O_6$ ceramic did not react with Al at the sintering temperature.

4 Conclusions

The structure and microwave dielectric properties in $Ba_{1-x}Sr_xV_2O_6$ ($0.35 \le x \le 0.55$) ceramics have been studied in order to get a thermally stable microwave dielectric material with preferable dielectric properties. XRD patterns confirmed that all the specimens formed a solid solution of $Ba_{1-x}Sr_xV_2O_6$ with orthorhombic structure. Near-zero τ_f value can be achieved by appropriately adjusting the x-value on account of the negative τ_f value of SrV_2O_6. A thorough study of microwave dielectric properties of the $Ba_{0.5}Sr_{0.5}V_2O_6$ ceramics depending on sintering temperatures indicated that $Ba_{0.5}Sr_{0.5}V_2O_6$ sintered at 625 °C exhibited a thermal stable dielectric owing near-zero τ_f along with $\varepsilon_r \sim 11.5$ and Q×f ~ 14 100 GHz. Meanwhile, the $Ba_{0.5}Sr_{0.5}V_2O_6$ ceramics showed good chemical compatibility with Al electrode at 625 °C. These merits make it a promising material for ULTCC applications.

Acknowledgements This work is supported by the National Natural Science Foundation of China (Grant No. 51402235). China's Postdoctoral Science Foundation (Grant No. 2015M582696), and by Shaanxi Province Postdoctoral Science Foundation.

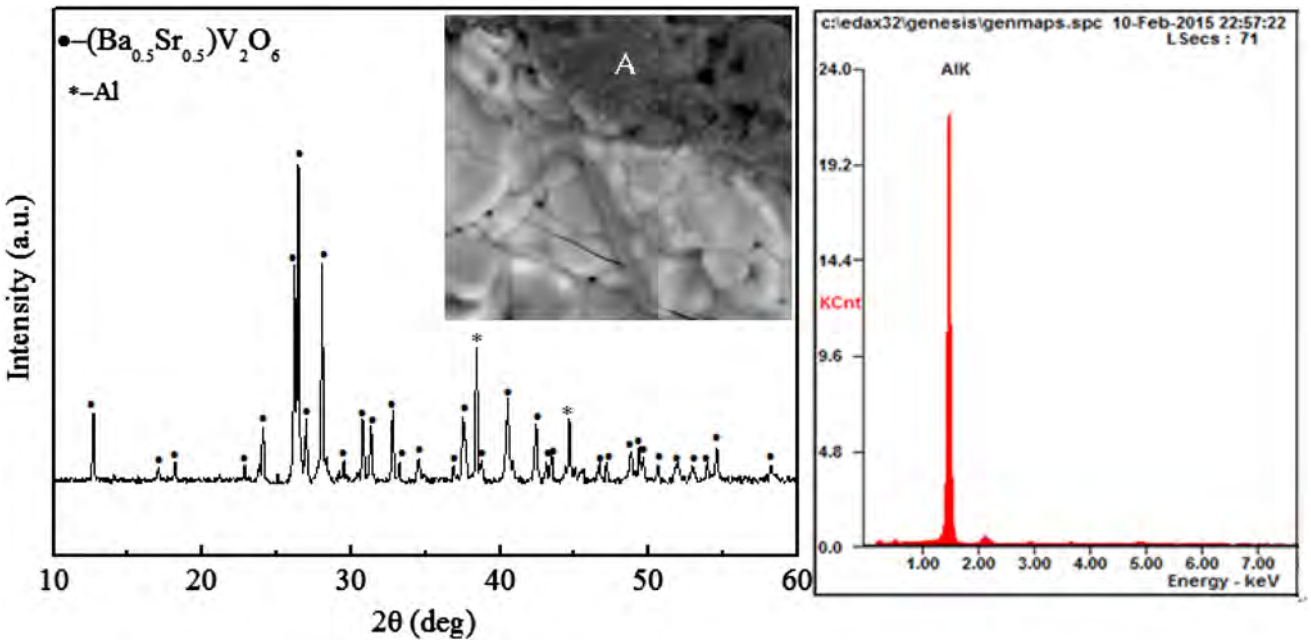

Fig. 5 XRD patterns and cross-section SEM image of the $Ba_{0.5}Sr_{0.5}V_2O_6$ ceramics after co-firing with 20 wt% Al at 625 °C

References

1. L.X. Pang, D. Zhou, Z.M. Qi, W.G. Liu, Z.X. Yue, I.M. Reaney, J. Mater. Chem. C **5**, 2695 (2017)
2. H.P. Braun, A. Mehmood, H.R. Zhang, S.B. Heidary, C. Randall, M.T. Lanagan, I.M. Reaney, J. Eur. Ceram. Soc. **37**, 2137 (2017)
3. W. Jin, W.L. Yin, S.Q. Yu, M.J. Tang, Mater. Lett. **173**, 47 (2016)
4. X.H. Ma, S.H. Kweon, S. Nahm, C.Y. Kang, S.J. Yoon, J. Eur. Ceram. Soc. **37**, 600 (2017)
5. J. Varghese, M.T. Sebastian, H.L. Jantunen, ACS Sustain. Chem. Eng. **4**, 3897 (2016)
6. R.R. Turnmala, J. Am. Ceram. Soc. **74**, 895 (1991)
7. H.T. Yu, J.S. Liu, W.L. Zhang, S.R. Zhang, J Mater Sci. **26**, 9414 (2015)
8. M.T. Sebastian, H. Wang, H.L. Jantunen, Curr. Opin. Solid State Mater. Sci. **20**, 151 (2016)
9. M. Udovic, M. Valant, D. Suvorov, J. Eur. Ceram. Soc. **21**, 1735 (2001)
10. G.K. Choi, J.R. Kim, S.H. Yoon, S.K. Hong, J. Eur. Ceram. Soc **27**, 3063 (2007)
11. E. K. Suresh, A. N. Unnimaya, A. Surjith, R. Ratheesh, Ceram. Int. **39**, 3635 (2013)
12. L. Fang, C.X. Su, H.F. Zhou, H. Zhang, J. Am. Ceram. Soc. **96**, 688 (2013)
13. D. Zhou, L.X. Pang, D.W. Wang, I.M. Reaney, J. Mater. Chem. C **4**, 5357 (2016)
14. C.H. Su, Y.S. Wang, C.L. Huang, J. Alloys Comp. **641**, 93 (2015)
15. H. F. Zhou, F. He, X. L. Chen, L. Fang, J. Mater Sci. **25**, 1480 (2014)
16. D. Zhou, L.X. Pang, Z.M. Qi, Q.P. Wang, C.A. Randall, Inorg. Chem. **53**, 1048 (2015)
17. G.G. Yao, P. Liu, J.J. Zhou, H.W. Zhang, J. Eur. Ceram. Soc. **34**, 2983 (2014)
18. S.E. Kalathil, A. Neelakantan, R. Ratheesh, J. Am. Ceram. Soc. **97**, 1530 (2014)
19. E. K. Suresh, K. Prasad, N. S. Arun, R. Ratheesh, J. Electron. Mater. **45**, 2996 (2016)
20. U.A. Neelakantan, S.E. Kalathil, R. Ratheesh, Eur. J. Inorg. Chem. **2**, 305 (2015)
21. R. Umemura, H. Ogawa, A. Yokoi, H. Ohsato, A. Kan, J. Alloys Compd. **424**, 388 (2006)
22. M.R. Joung, J.S. Kim, M.E. Song, S. Nahm, J. Am. Ceram. Soc. **92**, 3092 (2009)
23. Y. Zhang, Y.C. Zhang, M.Q. Xiang, J. Eur. Ceram. Soc. **36**, 1945 (2016)
24. Y. Wang, R.Z. Zuo, Ceram. Int. **42**, 10801 (2016)
25. B. Schnuriger, R. Enjalbert, J. M. Savariault, J. Galy, J. Solid. State Chem. **95**, 397 (1991)
26. S. Hasen, J. Nilsson, ActaChem. Scand **50**, 512 (1996)
27. J.Z. Gong, H.F. Zhou, F. He, X.L. Chen, L. Fang, Ceram. Int. **41**, 11125 (2015)
28. U.A. Neelakantan, S.E. Kalathil, R. Ratheesh, Eur. J. Inorg. Chem. **2015**, 305 (2015)
29. X. S. Jiang, H.L. Pan, Z.B. Feng, H.T. Wu, J. Mater. Sci-Mater. El. **27**, 10963 (2016)
30. H.T. Chen, Z. Xiong, Y. Yuan, B. Tang, S.R. Zhang, J. Mater. Sci-Mater. El. **27**, 10951 (2016)
31. H.J. Lee, K.S. Hong, S.J. Kim, Mater. Res. Bull. **32**, 847 (1997)
32. N. Khobragade, E. Sinha, S.K. Rout, M. Kar, Ceram. Int. **39**, 9627 (2013)